Downloaded 02/04/19 to 68.97.115.26. Redistribution subject to SEG license or copyright; see Terms of Use at http://library.seg.org/

In-context interpretation: Avoiding pitfalls in misidentification of igneous bodies in seismic data

Lennon Infante-Paez[1] and Kurt J. Marfurt[1]

Abstract

In the past few decades, many exploration wells have been drilled into igneous rocks because of their similar seismic expressions to common exploration targets, such as carbonate mounds, sheet sands, and sand-prone sinuous channels. In cases in which interpreters cannot clearly delineate sedimentary features such as channels or fans, the interpretation may be driven primarily by bright spot anomalies, in which a poor understanding of the wavelet polarity may lead to an erroneous interpretation. Although many wells drilled into igneous rocks are based on the interpretation of 2D seismic data, misinterpretation still occurs today using high-quality 3D seismic data. To address this challenge, we analyze the seismic expression of andesitic volcanoes in the Taranaki Basin, New Zealand and use it to help understand misinterpreted igneous bodies in different parts of the world. Then, we develop an in-context interpretation workflow in which the seismic interpreter looks for key clues above, below, and around the target of interest that may alert the interpreter to the presence of igneous rocks.

Introduction

Although igneous rocks are common in Australia, Argentina, Brazil, the UK-Norway continental margin, Indonesia, New Zealand, China, and other oil provinces around the world, there is only limited documentation of the seismic expression of igneous bodies. Furthermore, more than 90% of the documentation that does exist is focused on mafic intrusions (mainly sills), such." as those described by Planke et al. (1999), Hansen and Cartwright (2006), Miles and Cartwright (2010), Klarner and Klarner (2012), Schofield et al. (2017), Holford et al. (2013), Jackson et al. (2013), Alves et al. (2015), Magee et al. (2016), Cortez and Santos (2016), McLean et al. (2017), Hafeez et al. (2017), Gao et al., (2017), Schmiedel et al. (2017), Infante-Paez and Marfurt (2017), and more recently by Rabbel et al. (2018) and Infante-Paez (2018). Most of these studies focus on the mechanisms of magma emplacement into the sedimentary overburden, the associated deformation, and the magmatic plumbing system. Moreover, the published literature is biased toward the European side of the North Atlantic continental margin (UK-Norway), Australia, and Brazil. Only a few studies directly address the identification of igneous rocks in seismic data (Klarner and Klarner, 2012) to avoid misinterpreting them as common sedimentary exploration targets.

Several publications examine igneous bodies that mimic common sedimentary exploration targets such as carbonate mounds, sinuous channels, and hydrocarbon bright spots. For example, according to Mark et al. (2018), in the Faroe-Shetland Basin, Northeast Atlantic, exploration companies targeting Carboniferous/Devonian, Jurassic, and Lower Cretaceous sandstones have drilled mafic igneous sills based on high amplitudes observed in seismic data (Figure 1). Similarly, using a legacy 2D seismic survey from 1982, in the Taranaki Basin, New Zealand, the Arawa-1 well drilled a bright spot on a structural high as a secondary target. This bright spot was andesitic volcanic tuff, probably sourced by subaqueous flows of adjacent Miocene volcanoes (Figure 2). In the San Jorge Basin, Argentina, exploration/development wells targeting sand-prone meandering channels have drilled mafic lava flows with well-developed meander loops, filling a preexisting meander valley (Figure 3). In the Bass Basin, Australia, basaltic volcanoes were drilled by at least two exploration wells, which were originally intended to test the hydrocarbon potential of a Miocene "reef complex" at 790 m (Holford et al., 2017; Reynolds et al., 2018; Figure 4).

Given these examples where clastic, carbonate, and igneous bodies exhibit similar characteristics, it is clear that one should not limit an interpretation solely on the geometry or seismic expression of a preconceived or desired model because in doing so, we become victims of confirmation bias. Krueger and Funder (2004) define confirmation bias as "actively looking for opinions and evidences that support one's own beliefs or hypotheses." See Bond et al. (2007) for examples of confirmation bias in seismic interpretation. According to the authors from the mentioned examples above, we can

[1]The University of Oklahoma, School of Geology and Geophysics, Norman, Oklahoma, USA. E-mail: lennoninfante@ou.edu; kmarfurt@ou.edu.
Manuscript received by the Editor 11 April 2018; revised manuscript received 25 June 2018; published ahead of production 13 August 2018; published online 26 October 2018. This paper appears in *Interpretation*, Vol. 6, No. 4 (November 2018); p. SL29–SL42, 22 FIGS.
http://dx.doi.org/10.1190/INT-2018-0076.1. © 2018 Society of Exploration Geophysicists and American Association of Petroleum Geologists. All rights reserved.

Downloaded 02/04/19 to 68.97.115.26. Redistribution subject to SEG license or copyright; see Terms of Use at http://library.seg.org/

note how confirmation bias was unconsciously executed in the Faroe Shetland, New Zealand, and Australia case studies (Figures 1, 2, and 4), where the explorationists believed to have found in their seismic data the expression of their conceptual geologic target. Counterintuitively, the best way for an interpreter to avoid confirmation bias is to gain a deeper understanding of features they are not interested in drilling, which in this paper is a better understanding of the seismic expression and geomorphology of igneous intrusive and extrusive bodies.

Our primary objective in documenting the seismic expression of igneous bodies is to alert the interpretation community to potential pitfalls when exploring for hydrocarbons in a sedimentary basin affected by volcanism, e.g., misinterpreting igneous features as hydrocarbon bright spots, carbonate mounds, or meandering channels. Perhaps the best way to avoid such pitfalls is to do an in-context interpretation. This is essentially the identification of subtle or potential architectural elements of igneous systems (Klarner et al., 2006; Klarner and Klarner, 2012). Specifically, the presence of deeper sills, associated forced folds, velocity pull ups, and poorly imaged vertical dikes near shallower volcanic vents serve as key indicators that the mounds or channel-like features may not be carbonate buildups or channelized turbidites.

We acknowledge that event polarity, interval velocity, and amplitude variation with offset are also techniques commonly used in seismic analysis when suspected volcanics are involved. Nevertheless, sometimes even these techniques cannot distinguish between a mafic volcanic edifice or a prospective carbonate mound (Klarner and Klarner, 2012). Therefore, we focus our efforts on the identification of architectural elements of igneous systems and their spatial relationships.

For this reason, our goal is to document how igneous rocks appear in seismic data. Specifically, this study documents the seismic expression of andesitic (intermediate magma composition) volcanoes in the Taranaki Basin, New Zealand, which were drilled by exploration wells beginning in the 1980s. We link the presence of igneous sills, disruption of reflections, and forced folds below and around volcanoes to the same magmatic episode responsible for building the volcanic edifices. Finally, we propose an in-context interpretation workflow, in which the seismic interpreter looks for key clues above, below, and around the target of interest that may indicate the presence of igneous rocks.

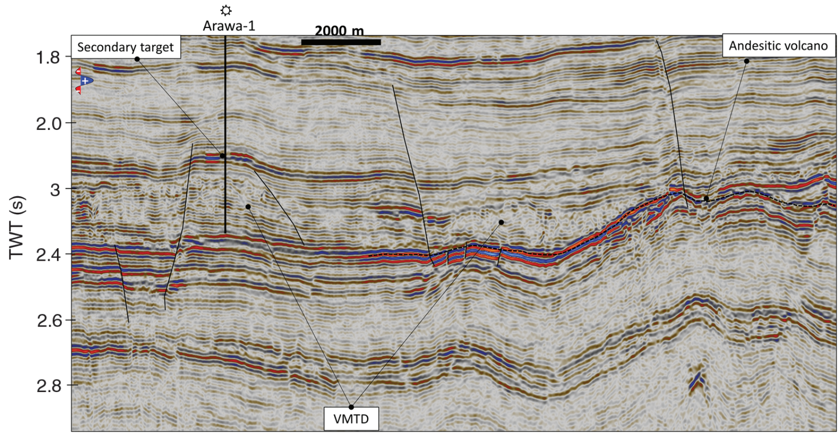

Figure 2. Exploration well Arawa-1 drilling into a bright spot (andesitic volcanic pile). Notice the andesitic volcano on the right side. VMT, volcanic mass transport deposit. Seismic data courtesy of New Zealand Petroleum and Minerals (NZP&M).

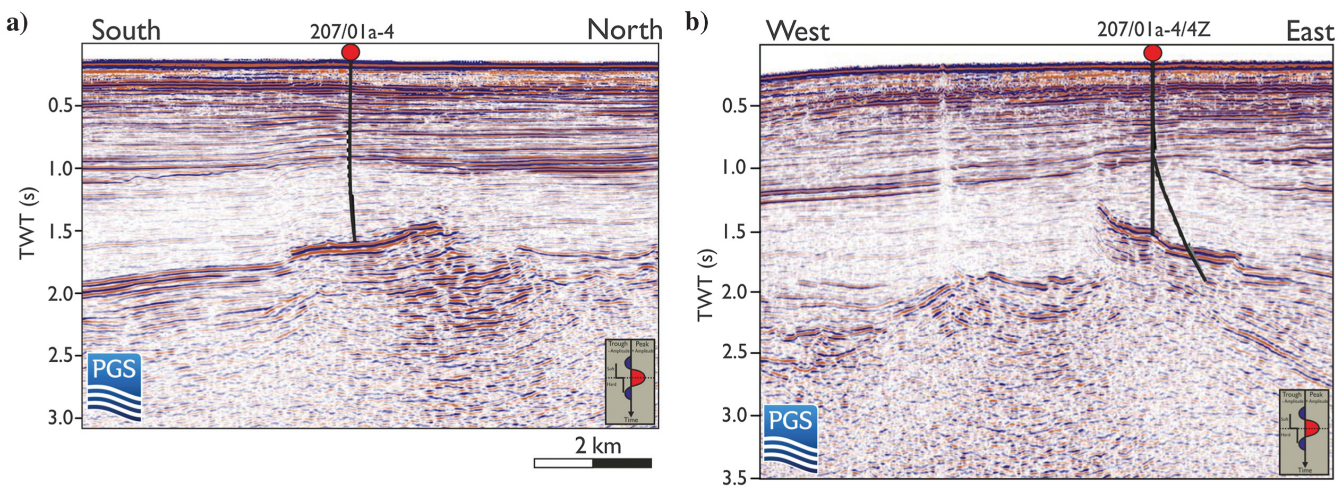

Figure 1. Exploration well drilling into mafic igneous sills. Seismic data courtesy of PGS. Reprinted from Mark et al. (2018), with permission from Elsevier.

Downloaded 02/04/19 to 68.97.115.26. Redistribution subject to SEG license or copyright; see Terms of Use at http://library.seg.org/

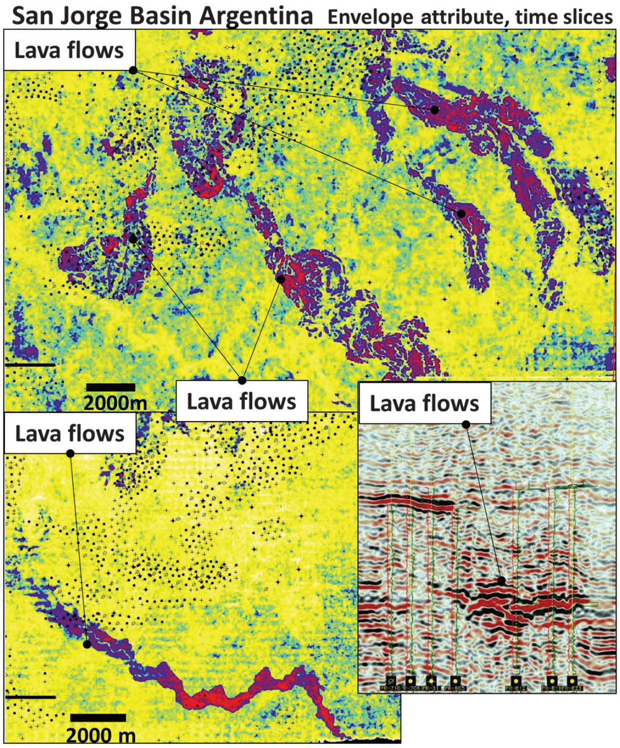

Figure 3. Envelope attributes in time slices and vertical amplitude section showing development wells drilled into channel-like features. The wells ended up drilling basaltic lava flows that were confined to meander valleys. Figure courtesy of Luis Vernengo, Pan American Petroleum.

Tectonic background of the Taranaki Basin, New Zealand

The focus area of our study is in the Northern Graben of the Taranaki Basin, New Zealand. A summary of the tectonic history of this basin is described by Infante-Paez and Marfurt (2017). Although very extensive and complex, the evolution of the Taranaki Basin can be briefly summarized in three major phases of deformation: the (1) Cretaceous to Paleocene (approximately 84–55 Ma) extension, (2) Eocene to Recent (approximately 40–0 Ma) shortening, and (3) Late Miocene to Recent (approximately 12 Ma) extension (Giba et al., 2010). The Late Cretaceous extension was responsible for the breakup of Gondwana (King and Thrasher, 1992, 1996), whereas shortening in the Taranaki Basin is thought to have occurred as a consequence of the subduction of the oceanic Pacific plate with the continental Australian Plate (DeMets et al., 1994; Beavan et al., 2002). The last phase of deformation was Miocene and younger extension accompanied by volcanism that commenced at approximately 16 Ma and continues at Mt. Taranaki today (Neall et al., 1986; Hayward et al., 1987; Bergman et al., 1992; King and Thrasher, 1992). These volcanic centers are mainly stratovolcanoes, of mostly low-medium K andesitic composition and, together with their north–northeast-trending alignment parallel to the late Miocene subduction margin (Figure 5), suggest that magmas are derived from the subducting Pacific Plate beneath the basin (Bergman et al., 1992).

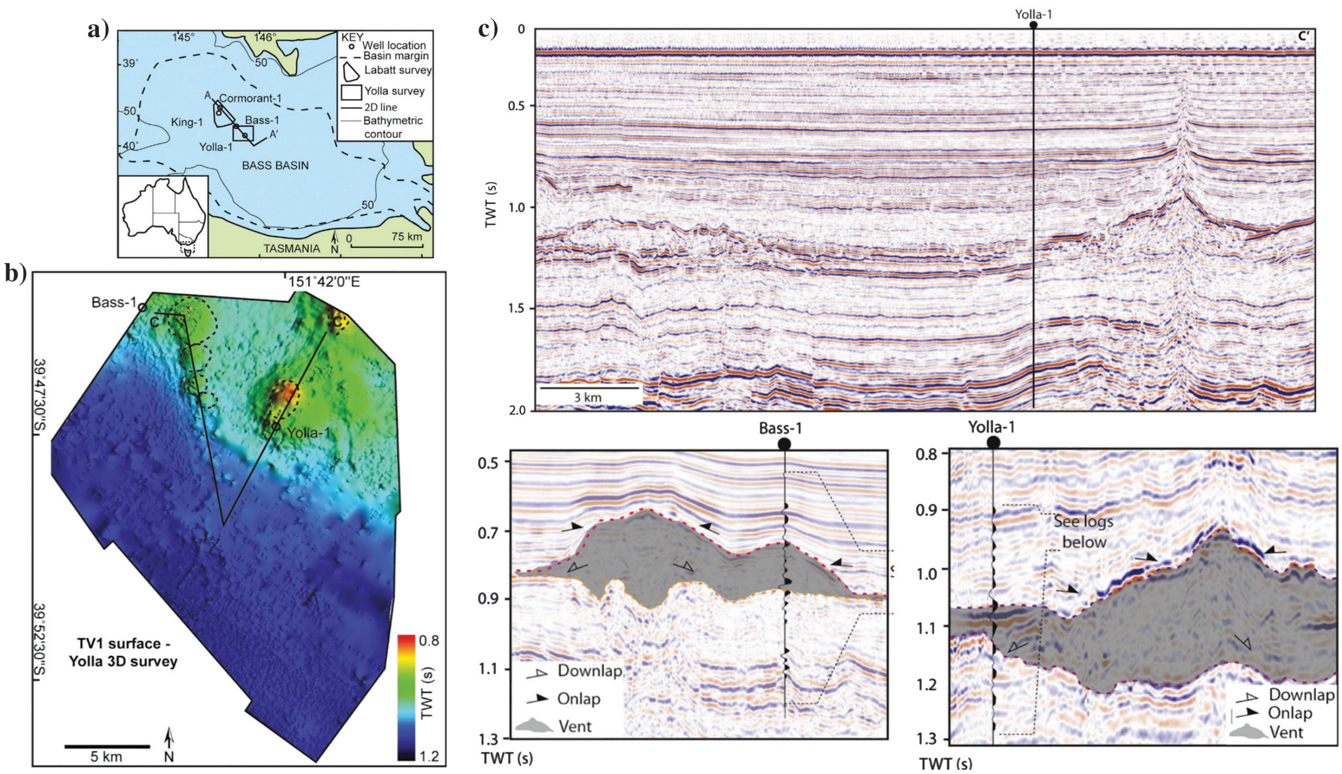

Figure 4. Vertical amplitude sections showing exploration wells drilled into mound-like features. The wells drilled a basaltic volcano rather than a carbonate buildup. The map on the bottom left is the top of the volcanic units. Notice the dome-like shape. After Reynolds et al. (2018).

Downloaded 02/04/19 to 68.97.115.26. Redistribution subject to SEG license or copyright; see Terms of Use at http://library.seg.org/

Extrusive igneous bodies in the Taranaki Basin, New Zealand

Andesitic volcanoes

Some of the andesitic stratovolcanoes that form the Mohakatino Volcanic Belt (MVB) described by Bergman et al. (1992) and King and Thrasher (1996) were penetrated in the early to late 1980s by exploration wells: Tua-Tua-1, Mangaa-1, Te-Kumi-1, and Kora-1, 2, 3, and 4 (Figures 6, 7, and 8). According to well-completion reports, these volcanoes were built from the mid-bathyal paleo seafloor (800–1300 m).

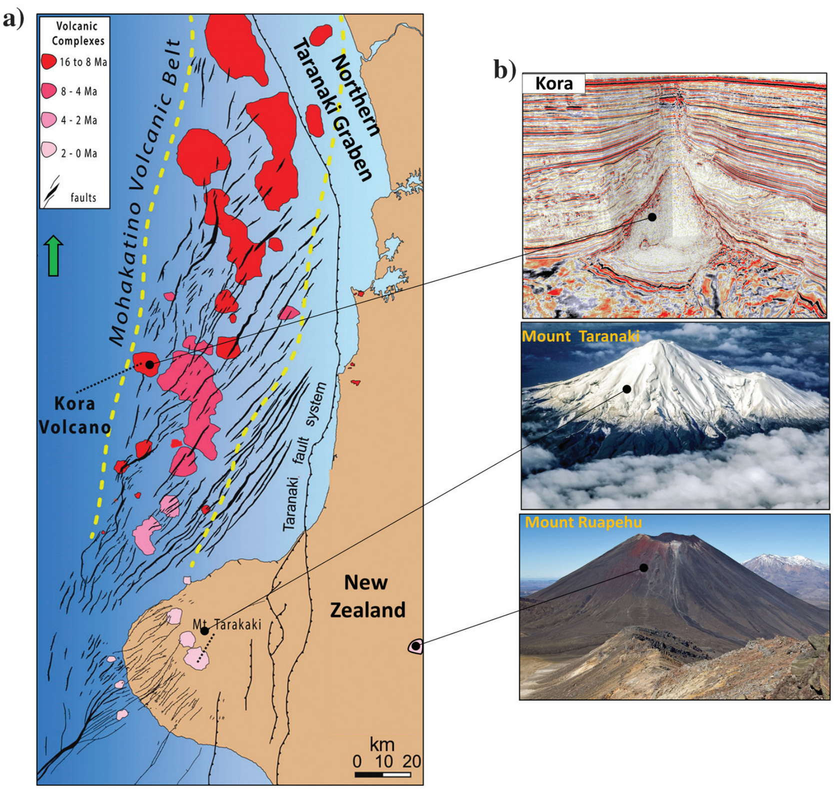

Figure 5. (a) Location map of New Zealand showing the Taranaki Basin and the size and distribution of the MVB in red. (b) Onshore younger andesitic volcanoes and 3D seismic sections showing the Kora Volcano. After Giba et al. (2013) and Bischoff et al. (2017).

Seismic imaging of the volcanoes clearly depends on the data quality, with (post-2006) 3D surveys providing superior images to 2D surveys acquired in 1995 (Figure 9). On time-migrated seismic data, they show a trapezoidal to mounded geometry with moderate- to high-amplitude continuous reflections on the flanks, and a chaotic "salt and pepper" internal configuration (Figures 6–9). Wells that penetrate these volcanic cones encounter sequences of andesitic tuff to poorly sorted lapilli and breccias, with plagioclase and hornblende being major mineral components along with clay and rock fragments (Awatea-1, Te-Kumi-1, Tua-Tua-1, and Kora-1, 2, 3, and 4 well-completion reports).

The exact lateral extent of any given volcano is difficult to define because of insufficiently dense 2D data grid; specifically, the 2D seismic lines may slice the volcanic cone on its flanks, rather than the summit, masking its true height and extent. Given this disclaimer, we find the volcanoes to be approximately 4–5 km in radius and rise between 500 and 800 m above the paleo seafloor.

Whether analyzing 2D or 3D seismic surveys, the onlap of sediments onto the volcano flanks show that they were either volcanic islands or seamounts, where the age of the onlapping sediments indicates the relative age of the igneous bodies. Giba et al. (2013) use biostratigraphic dating of the sediment layers provided by offshore Taranaki Basin exploration wells to constrain the age of the Tua-Tua, Te-Kumi, Mangaa, and Kora Volcanoes (Figures 6–9) to be between 33.7–10, 12–8, 12–5.5, and 12–5.5 Ma, respectively.

The well control through several cone- to mound-like structures seen on seismic data calibrates the characteristic external and internal seismic features of andesitic volcanoes, which can be used to interpret similar nearby undrilled seismic features (Figure 10). The volcanoes exhibit a cone to mounded structure ranging from 500 to 100 ms in two-way traveltime (TWT). Although seamounts may retain their cone shape, subaerially exposed volcanic islands will be eroded, resulting in a truncated cone to a more mounded appearance. Steeply dipping flanks (>20°), internal heterogeneity, and higher velocity than the surrounding sediments give rise to imaging problems, resulting in a nearly complete disruption of the continuity of the reflections immedi-

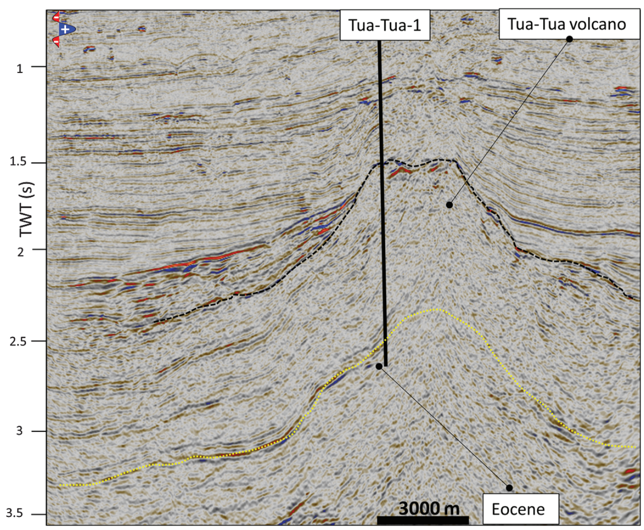

Figure 6. Vertical seismic amplitude section from P95 2D seismic survey showing Well Tua-Tua-1 drilling an andesitic volcano, the Tua-Tua Volcano. Seismic data courtesy of NZP&M.

Downloaded 02/04/19 to 68.97.115.26. Redistribution subject to SEG license or copyright; see Terms of Use at http://library.seg.org/

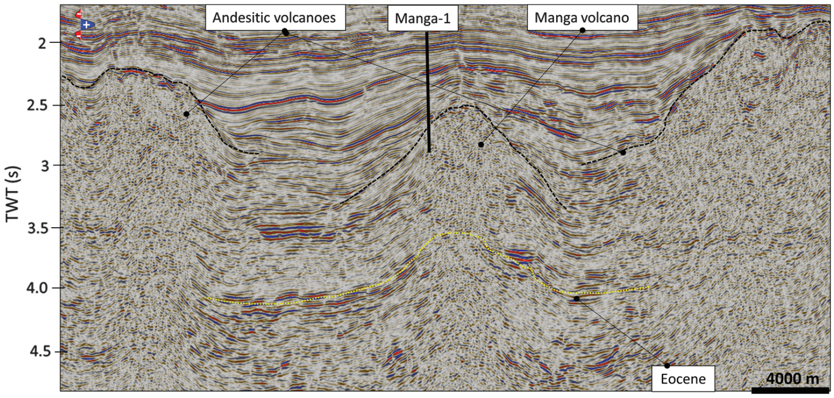

Figure 7. Vertical seismic section from P95 2D seismic survey showing well Manga-1 drilling an andesitic volcano, the Manga Volcano. Seismic data courtesy of NZP&M.

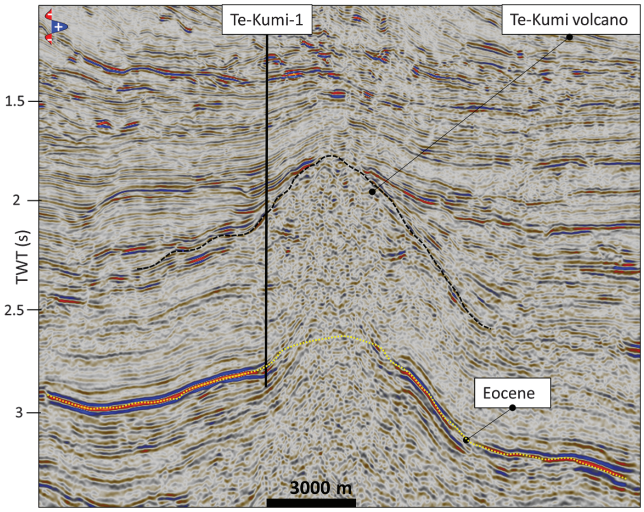

Figure 8. Vertical seismic section from P95 2D Survey showing well Te Kumi-1 drilling an andesitic volcano, Te-Kumi Volcano. Seismic data courtesy of NZP&M.

ately below the volcanoes. Analyzing a 3D seismic survey from the Santos Basin, offshore Brazil, Cortez and Santos (2016) call a similar lack of continuity of the reflections "shadow zones." In seismic surveys from the Taranaki Basin, this disruption continues horizontally 3000–5000 m below the paleo seafloor at the time of eruption, which is inconsistent with vertical pipe feeder models ranging only hundreds of meters in diameter C. K. Morley (personal communication, 2018). Examining the deeper reflections below the volcanic cones, Figures 6–10 show deeper reflections that are pulled up along with those concordant with the top of the volcano surface. For this reason, although velocity heterogeneity may lead to a poor image, most of the doming is structural (Figure 11), rather than a velocity pull-up artifact.

Intrusive igneous bodies in the Taranaki Basin

Igneous sills

Although not extensively documented because they are not exploration objectives, the most common features related to igneous bodies seen in seismic data are intrusive sills (Planke et al., 1999; Hansen and Cartwright, 2006; Miles and Cartwright, 2010; Holford et al., 2012; Jackson et al., 2013; Alves et al., 2015; Cortez and Santos, 2016; Magee et al., 2016; Gao et al., 2017; Hafeez et al., 2017; Infante-Paez and Marfurt, 2017; McLean et al., 2017; Naviset et al., 2017; Schofield et al., 2017; Mark et al., 2018; Infante-Paez, 2018; C. K. Morley (personal communication, 2018); Rabbel et al., 2018).

A good example of episodic Miocene magmatism in the Taranaki Basin is the Kora Volcano. Vertical sections around this edifice show multiple high-amplitude, continuous (2–3 km in diameter) saucer-shaped reflections below the volcano that cut across the stratigraphy (Figure 11). Figure 12 illustrates the spatial distribution

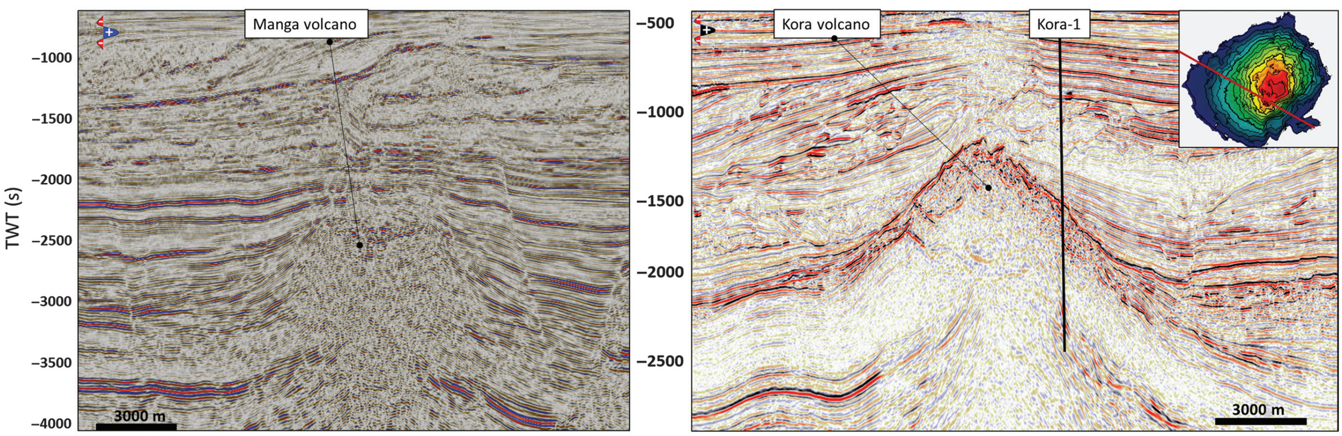

Figure 9. Signal-to-noise comparison between (a) legacy 2D ES-89 seismic survey from 1989 and (b) modern 3D Kora 3D 2006 seismic survey. Notice the higher quality image of the Kora Volcano compared with the Manga Volcano. Seismic data courtesy of NZP&M.

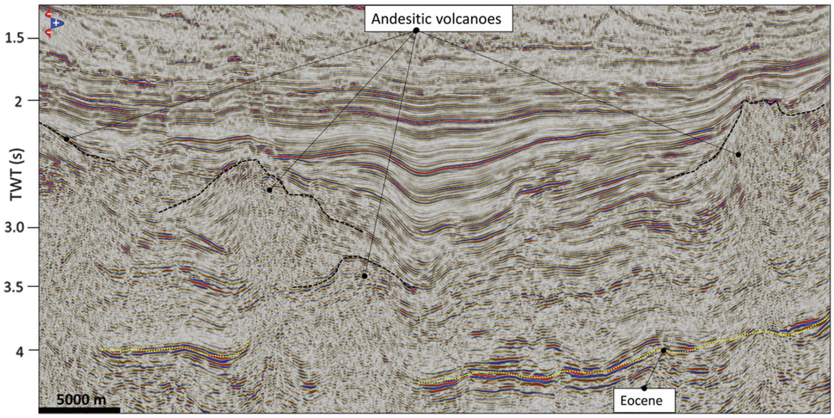

Figure 10. Seismic section from P95 2D seismic survey showing several undrilled mound-like structures interpreted as andesitic volcanoes. Seismic data courtesy of NZP&M.

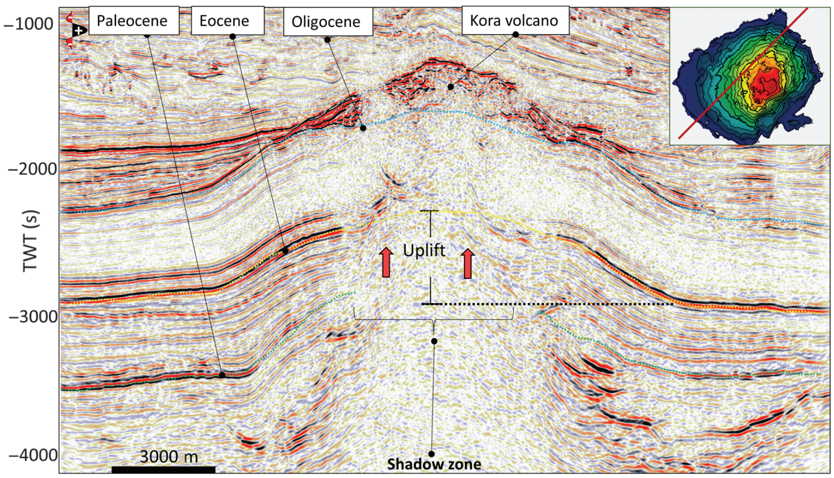

Figure 11. Seismic section from Kora 3D seismic survey showing the Kora Volcano and the uplift of the reflections beneath the edifice as well as the disruption of the reflections (shadow zone). Seismic data courtesy of NZP&M.

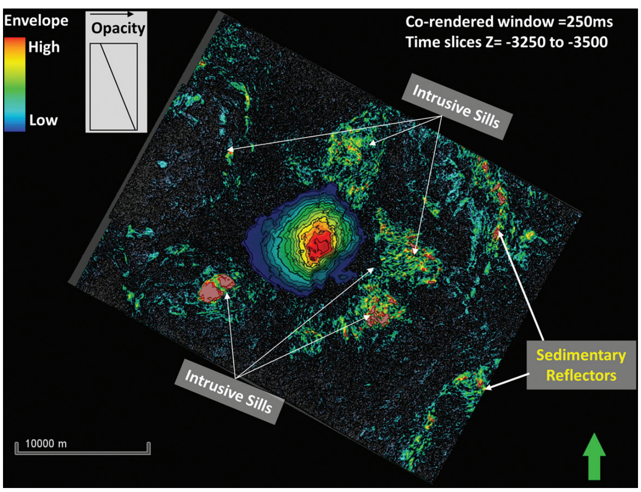

Figure 12. Map view of the envelope attribute in a corendered window of 250 ms showing spatial distribution of igneous sills around the Kora Volcano. After Infante-Paez and Marfurt (2017). Seismic data courtesy of NZP&M.

of these reflections around the Kora Volcano using a set of corendered time slices through the instantaneous envelope attribute that shows the semicircular distribution of these high-amplitude reflections below and around the volcano. The spatial relationship to the Kora Volcano supports the hypothesis that they are igneous bodies related to the same magmatic event that created the volcanic edifice in the Early-Middle Miocene (Bergman et al., 1992; Giba et al., 2013). These saucer-shaped, high-amplitude reflections exhibit the same morphology as those documented by DuToit (1920), Planke et al. (1999), and others from the rifted European side of the North Atlantic margin, Brazil, and Australia, where rifting facilitates mafic magmatism due to decompression and partial melting of the ultramafic mantle. Furthermore, Sarkar and Marfurt (2017) describe similar andesitic saucer-shaped sills drilled and logged on the way down to deeper turbidites in the Chicontepec Basin of eastern Mexico. Regardless of their composition, the appearance of these sills below Kora is similar to those formed due to extension and subduction-related magmatism. Given these morphological analogs in the mafic and intermediate provinces, we interpret the saucer-shaped high amplitudes in the Kora 3D survey to be sills (Figure 13). Furthermore, the host rocks into which these igneous bodies intrude may be of interest in hydrocarbon exploration. Figure 13 illustrates a vertical slice through a seismic amplitude section showing multiple approximately 2 km width sills and possible laccoliths that thermally modify the Paleocene source rock, such as described by Delpino and Bermudez (2009). In this scenario, heat from the sills places immature source rocks within the oil window. Igneous intrusion will produce contact metamorphism in the host rocks nearby the intrusion. These thermally altered rocks or "hornfels," such as those studied in outcrop by Liborius and Tazzo (2012) and Sarkar and Marfurt (2017) are often fractured, allowing hydrocarbons to migrate into the fractured igneous bodies (Delpino and Bermudez, 2009; Rodriguez Monreal et al., 2009; Senger et al., 2017; Rabbel et al., 2018)

Forced folds

Another possible parameter for identifying these igneous intrusions is deformation of the host rock. Jackson et al. (2013), Magee et al. (2014), Alves et al. (2015), and Schmiedel et al. (2017) report the occurrence of forced folds in seismic data. According to Schmiedel et al. (2017), most sills form folds because either the

Downloaded 02/04/19 to 68.97.115.26. Redistribution subject to SEG license or copyright; see Terms of Use at http://library.seg.org/

volume of the magma displaces that of the sediments or the intrusions are virtually incompressible with respect to the surrounding sedimentary rocks that do not compact, and therefore develop a structural dome. Figure 14a shows a sill complex in the Upper Cretaceous sequence and corresponding forced folds directly above the igneous intrusions (green arrows) as an example of postemplacement deformation. The wavelength of the fold appears to be linked to the lateral extent of the sills, whereas the amplitude of the fold seems to be related to the cumulative thickness. A crucial clue is that the amplitude of the fold deformation decreases stratigraphically upward, suggesting that the deformation occurred after the emplacement of the sill, probably due to differential compaction about the flanks (Schmiedel et al., 2017) and that the sill was emplaced in a zone of high pore-fluid volume that may have been fluidized to accommodate the volume of the magma. In contrast, Figure 14b shows an example of a forced fold, where terminations can be seen to lap onto the fold, suggesting syn-emplacement deformation, thereby defining the time of the initial intrusion (Hansen and Cartwright, 2006). Often, sills show evidence of syn- and postemplacement deformation and little to no deformation, respectively (Figure 14a, gray arrow). Magee et al. (2016) find that sometimes sill emplacement shows little to no deformation, suggesting fluidization. For this reason, although deformation is an indicator of the emplacement of most igneous bodies, not all igneous intrusions generate such features.

Igneous dikes

In magmatic systems, dikes are near-vertical intrusions commonly tens of meters thick and up to a few kilometers in extent (e.g., Thomson, 2007; Holdford et al., 2017; Reynolds et al., 2018) that cut across preexistent strata, usually intruding into zones of weakness such as faults and other mechanically weaker layers. The imaging of these igneous bodies in seismic data is challenging because seismic data will not image near-vertical features (Thomson, 2007), although recent advances in complex imaging indicate that in fact there are instances and settings in which nearly vertical features can be seismically imaged. Nevertheless, evidence of dikes can still be observed in seismic data (Holdford et al., 2017; Reynolds et al., 2018).

A series of near-vertical, narrow, low-amplitude reflections can be seen below the flanks of the Kora Volcano (Figure 15). These reflections create a pattern that is very difficult to distinguish from low signal-to-noise zones, where amplitudes may have been affected by absorption. However, they only cover a certain portion of the seismic section, between 2000 and 4000 ms TWT in Figure 15a and 15b. Additional evidence to the presence of these dikes is their spatial relationship to the flanks of the Kora Volcano, where reflections with a small conical shape appear (Figure 15). A coherence and dip magnitude stratal slice near the top of the Kora Volcano shows this feature to be semicircular (Figure 16a and 16b). Given the spatial and temporal relationship of these events, we interpret the near-vertical, narrow, and low-amplitude pattern to be near-vertical dikes that feed the small conical vents.

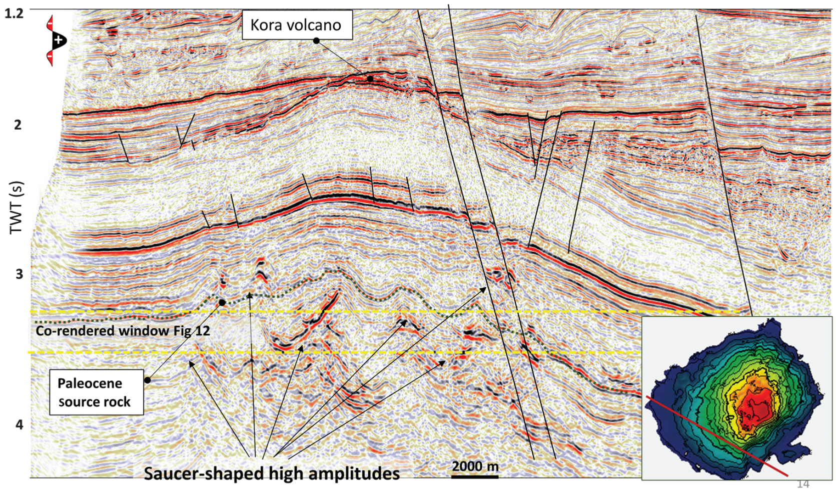

Figure 13. Vertical seismic section from the Kora 3D seismic survey showing interpreted saucer-shaped sills intruding into the Paleocene Waipawa marine source rock and possibly creating an atypical petroleum system, such as the one proposed by Del Pino and Bermudez (2009). After Infante-Paez and Marfurt (2017). Seismic data courtesy of NZP&M.

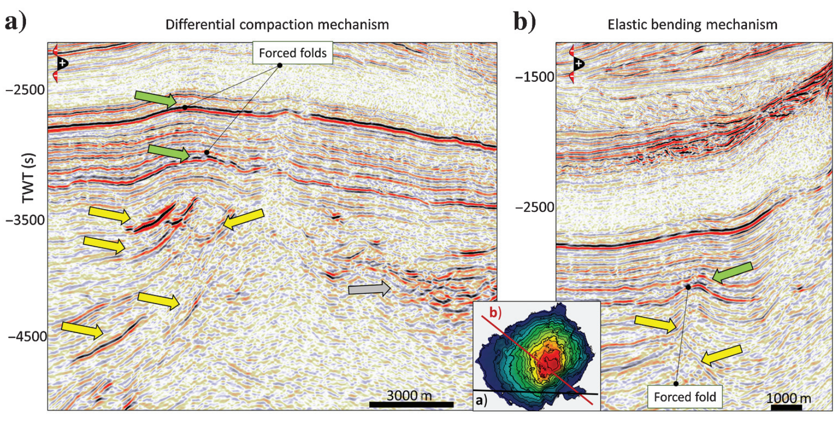

Figure 14. Vertical seismic sections from Kora 3D seismic survey illustrating different mechanisms of forced folds: (a) Postemplacement and (b) synemplacement. The yellow arrows point to the sills, the green arrows point to the forced folds, and the gray arrow points to a sill complex with no evidence of forced folding. Seismic data courtesy of NZP&M.

Downloaded 02/04/19 to 68.97.115.26. Redistribution subject to SEG license or copyright; see Terms of Use at http://library.seg.org/

This observation is consistent with the model proposed by Bischoff et al. (2017).

Implication for avoiding pitfalls in seismic interpretation

The images from the introduction show wells that penetrated mound- to cone-shaped structures and confirmed them as igneous volcanoes. In the absence of well control, the cone-to mound-like geometry is similar to carbonate reef exploration targets. In addition, Figure 17 shows examples of intrusive and extrusive igneous bodies that mimic the seismic expression of common sedimentary exploration targets. Based on their morphology alone, many interpreters will not be able to distinguish igneous bodies from their clastic counterparts (we encourage the reader to make an educated guess before reading the figure caption).

To try to distinguish between common exploration targets from Figure 17 and igneous bodies that mimic their geometry/morphology, we examine a few seismic amplitude sections of the Akira 2007 2D seismic survey acquired over the Taranaki Basin (Figure 18). The seismic data depict a series of cone- to mound-shaped features with chaotic internal reflection configurations and moderate to high amplitudes on their tops. Immediately below the mound-like features, there is a disruption in the reflections similar to those seen in the volcanoes in Figures 6–11. The mounds exhibit base lengths of approximately 2000 m with "steep" flanks and appear to be laterally interconnected. Based only on their geometry, these features are similar to "carbonate mounds" (Holdford et al., 2017; Reynolds et al., 2018) or even to mud volcanoes. The only unequivocal way to determine the composition of any of these mounds would be by drilling a well through it and to study an extracted core or cuttings. An alternative way would be to use potential field methods to differentiate between generally magnetic igneous rocks and nonmagnetic sedimentary rocks. However, remanent magnetization may confuse the interpretation (e.g., Pena et al., 2009), whereas diagenesis may result in magnetic volcanic tuff being converted to nonmagnetic montmorillonite (K. Marfurt, personal communication, 2017). An alternative and in-

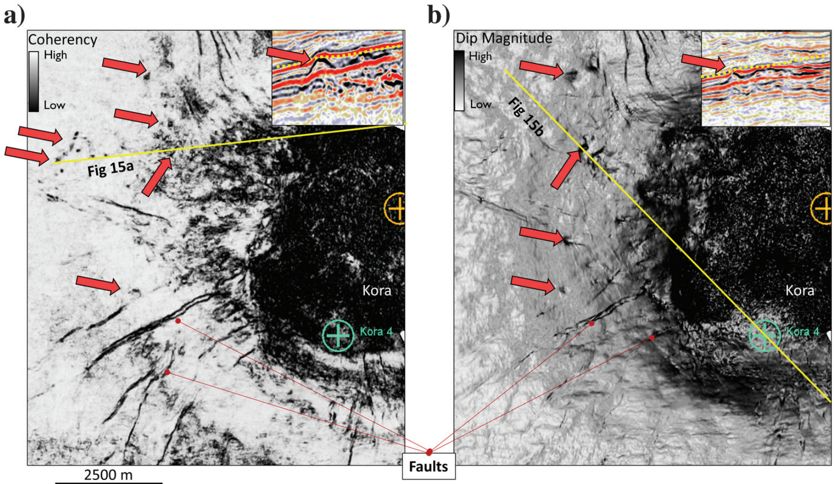

Figure 16. Map view of (a) coherency and (b) dip magnitude attributes extracted close to the top of the Kora Volcano. The reddish arrows point to small semicircular features in both attributes that represent the small cones. The dotted yellow line in the insert figure represents a reflection close to the base of Kora. Radial low coherency is normal faults and/or dikes. Seismic data courtesy of NZP&M.

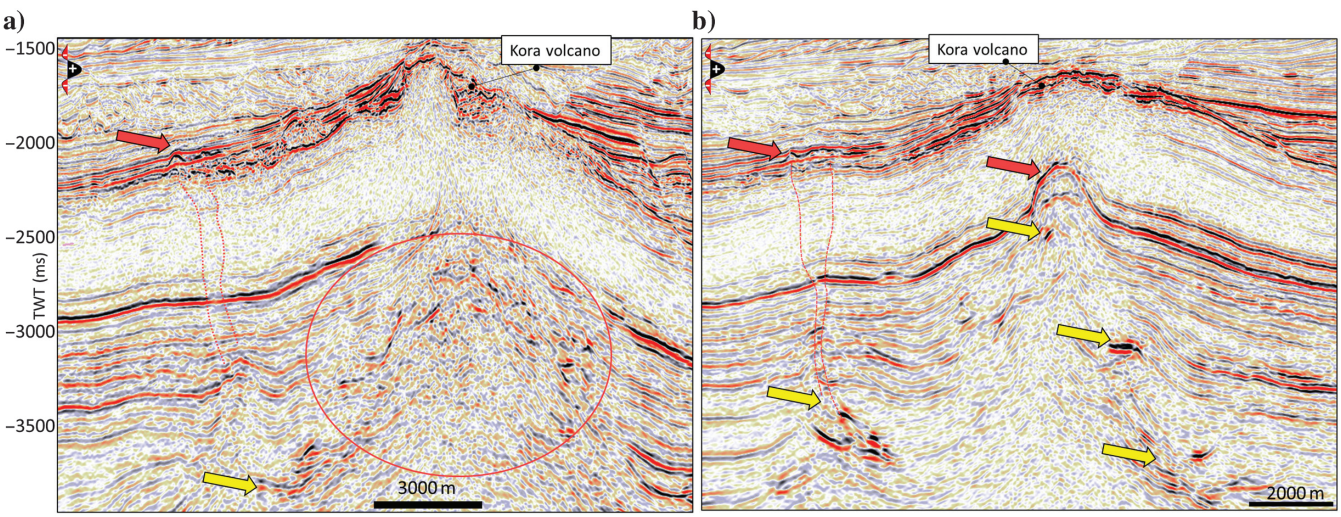

Figure 15. Seismic sections from thr Kora 3D survey showing interpreted igneous sills below the Kora Volcano (red polygon) and a subvertical low signal-to-noise zone above the sills (dotted reddish lines). Note the small-scale mound-cone structures on the flanks of Kora. (a and b) Different orientations. The yellow arrows point to the sills, whereas the reddish arrow points to the small cones and laccolith. The dotted reddish line represents the dikes. Seismic data courtesy of NZP&M.

Downloaded 02/04/19 to 68.97.115.26. Redistribution subject to SEG license or copyright; see Terms of Use at http://library.seg.org/

expensive method is to apply in-context interpretation. In this study, in-context interpretation refers to the concept implemented by H. Posamentier (personal communication, 2018), in which he looks at the pattern of the features of interest as well as the surrounding elements (e.g., what is below, what is above, and what is around).

In-context interpretation uses observations made at all scales and from all perspectives to generate a fully integrated, geophysically consistent, and geologically reasonable interpretation. It might be said, ideally, that this is what an interpreter always has done or should be doing. This approach develops naturally with experience and becomes standard practice for evaluation of competing interpretive models by helping to ensure that all available data and information are used to determine the most likely interpretive conclusions. In this paper, we have applied the in-context method to interpret the seismic expression of igneous rocks, and, based on this experience, we can envision the method being generally applicable to many different interpretation problems in a wide variety of geologic settings.

To illustrate the concept of in-context interpretation, we cite National Geographic's *Brain Games* TV show analogy illustrated in Figure 19. In this image, we see headshots of two former U.S. leaders. We can easily recognize former Vice President Dick Cheney on the left and former President George W. Bush on the right. Detailed examination of this image shows that they both have the same face (analogous to the ambiguous pattern of interest in geology, e.g., carbonate mounds, or volcanic mounds) with minor alterations. So, how is it that the same face gives two completely different persons (analogous to two different interpretations)? The key to differentiation lies in context (what is above, what is below, and what is around). In this case, the context is given by the glasses, the different hair style, hair, and skin color that allow us to distinguish former Vice President Cheney from former President Bush in Figure 19.

Applying the same in-context interpretation concept to Figure 18, we recognize other key clues that would

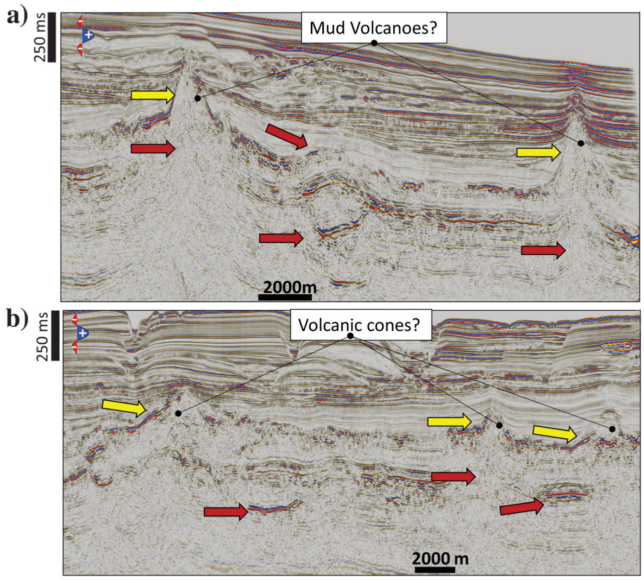

Figure 18 (a and b) Different seismic amplitude sections from Akira 2D seismic survey showing mound-like structures (yellow arrows) with similar geometry to the ones in the Bass Basin, Australia, in Figure 4. The red arrows represent clues for in-context interpretation. Seismic data courtesy of NZP&M.

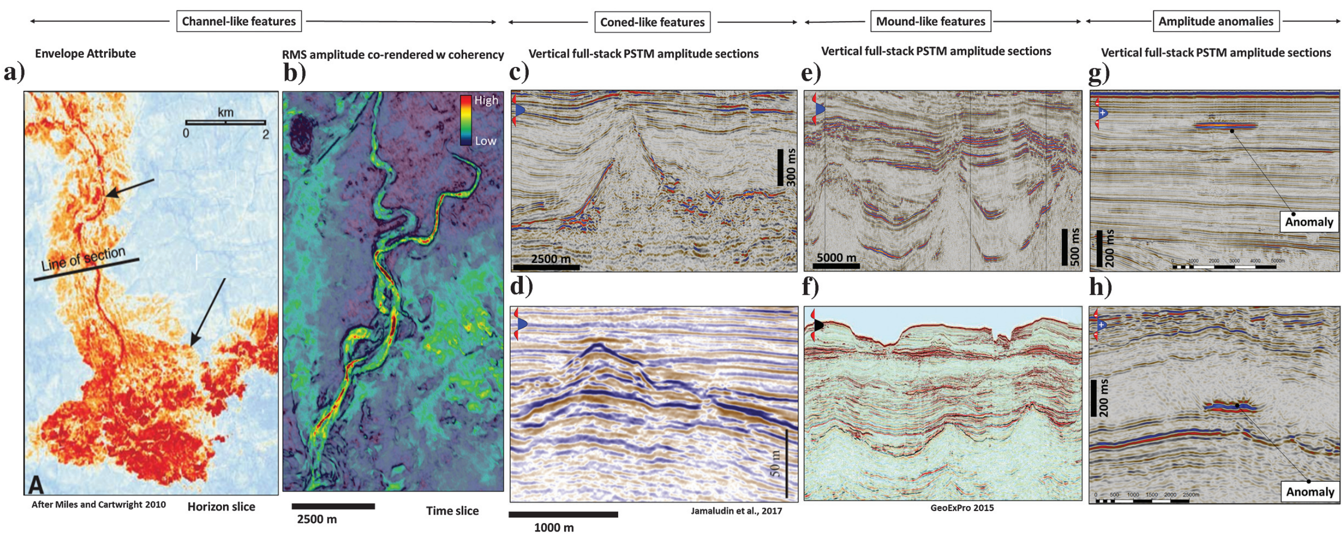

Figure 17. Geomorphology of igneous bodies. Vertical amplitude sections and horizon slices showing envelope attribute. There are a total of four different igneous bodies in this figure. Can you guess correctly which one they are before reading the rest of the caption? (a) Hybrid igneous flow. (b) Clastic channelized turbidites from Parihaka 3D; seismic survey courtesy of NZP&M. (c) Igneous volcano (andesitic) from Akira 2D seismic survey; seismic data courtesy of NZP&M. (d) Carbonate buildup. (e) Andesitic volcanoes from Parihaka 3D; seismic survey courtesy of NZP&M. (f) Jurassic-Early Cretaceous carbonate platform from Hand and Jackson (2015). (g) Bright spot (gas sand?) from Parihaka 3D; seismic survey courtesy of NZP&M. (h) Igneous sill, from Kora 3D; seismic survey courtesy NZP&M.

Downloaded 02/04/19 to 68.97.115.26. Redistribution subject to SEG license or copyright; see Terms of Use at http://library.seg.org/

help to infer the composition of the mound-like features. Among these clues are (1) saucer-shaped, high-amplitude sills around the mounds, (2) forced folds that are formed due to the emplacement of the sills (Hansen and Cartwright, 2006; Holford et al., 2012; Jackson et al., 2013; Magee et al., 2014, 2017; Infante-Paez and Marfurt, 2017; Schmiedel et al., 2017; Schofield et al., 2017) (red arrows), and (3) a subvertical, narrow, low-amplitude pattern in the section below these mounds that appears to disrupt the reflections for significant vertical distances (2250–3500 ms TWT, or more than 1 km) just below the mounds. Implementing an in-context interpretation, the presence of all these elements (saucer-shaped sills and forced folds in addition to the mounds) indicates an igneous composition of the mounds (Figure 20). In contrast, an interpretation driven by confirmation bias (Figure 21) in which the objective is to identify carbonate build-ups to test their reservoir potential might misinterpret the mound-like features to be pinnacle reefs, as appears to be the case documented by Holford et al. (2017) and Reynolds et al. (2018) in the Bass Basin, Australia.

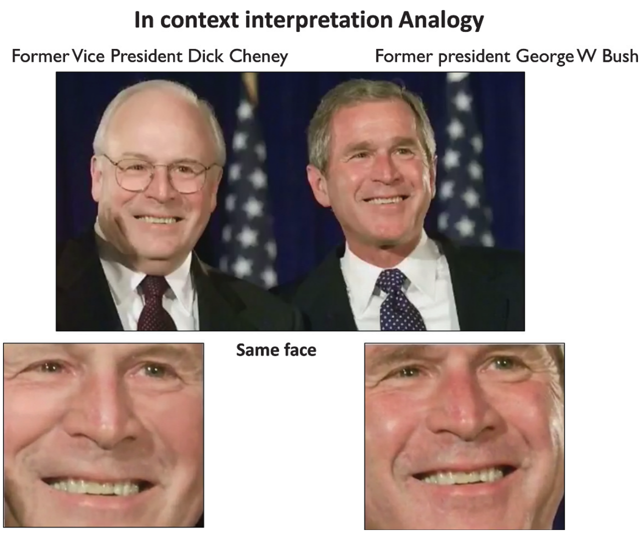

Figure 19. In-context interpretation analogy. Former U.S. leader headshot captured from the National Geographic TV show *Brain Games*.

Figure 22 summarizes our proposed workflow to avoid interpretation pitfalls in the presence of igneous intrusions and extrusions. The key to this workflow is not to stop when we find what we are looking for (finding the feature of interest from our conceptual geologic model), thereby confirming our bias. Rather, we perform in-context interpretation to try to match the evidence of the context to our exploration target, such as the igneous evidence found in Figure 18a and 18b. Further examination of the literature supports the igneous interpretation, where Jackson et al. (2013) and Magee et al. (2013) find similar features in the Ceduna subbasin of Australia to be volcanoes.

Weighing the evidence for igneous rocks in seismic data

Based on the analysis of igneous systems on the European side of the North Atlantic margin from the available literature and the multiple seismic surveys we have analyzed in the Taranaki Basin, we propose a ranking system in which different architectural elements of volcanic systems carry in-context "weight" when trying to identify igneous bodies in seismic data. This system assigns quantitative weighting factors to these elements as follows:

- We assign a factor of 1.00 to elements that are easy to identify in seismic data and that represent actual evidence of magmatism, such as igneous sills. High-amplitude, saucer-shaped, semicontinuous reflections representing igneous sills receive the highest weight because they have been observed in different basins with different tectonic settings around the world, where several publications report wells that have drilled these features and have penetrated igneous rocks (Alves et al., 2015; Naviset et al., 2017; Mark et al., 2018).
- We assign a factor of 0.75 to ambiguous elements that may disrupt reflections below a mound- to cone-shaped structure and may represent evidence of magmatism (igneous dikes); alternatively, these elements may be artifacts in seismic processing.
- We assign a factor of 0.50 to elements that can be present (forced folds), but whose absence does not indicate that an igneous system is not present.

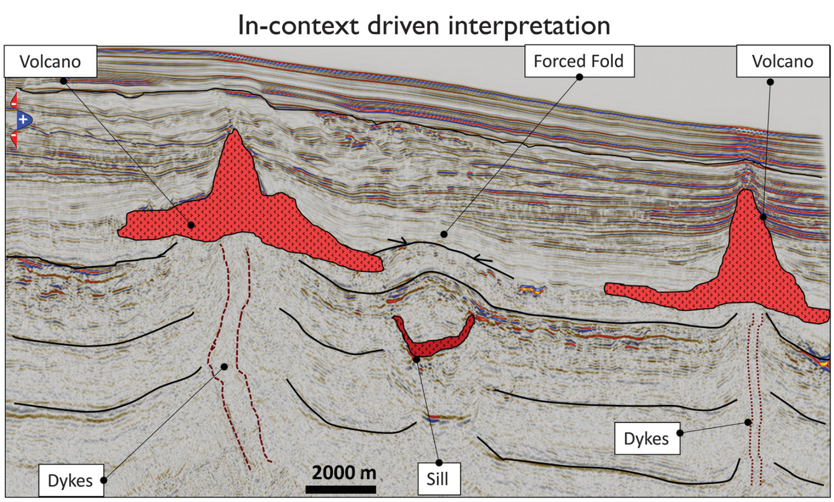

Figure 20. Interpreted vertical seismic section. In-context interpretation suggests the mound-like features are igneous volcanoes. Seismic data courtesy of NZP&M. Interpreted vertical seismic section from Figure 18a.

Downloaded 02/04/19 to 68.97.115.26. Redistribution subject to SEG license or copyright; see Terms of Use at http://library.seg.org/

- We assign a factor of 0.25 to small-scale elements of igneous systems that are difficult for inexperienced interpreters to identify, such as parasitic mounds, radial low signal-to-noise dikes, volcanic mass transport deposits, and pyroclastic flows from intermediate-composition volcanic eruptions.

These weights, properly calibrated by well control used in concert with an established prospect risking system, can be used as critical inputs to prospect risking and in deciding whether or not to recommend/approve drilling a well. We are unable to apply our quantitative ranking system in our study because we are not evaluating a prospect and therefore lack the necessary elements of a risking system. Nevertheless, we encourage feature work to apply this recommend ranking system whenever the necessary data are available.

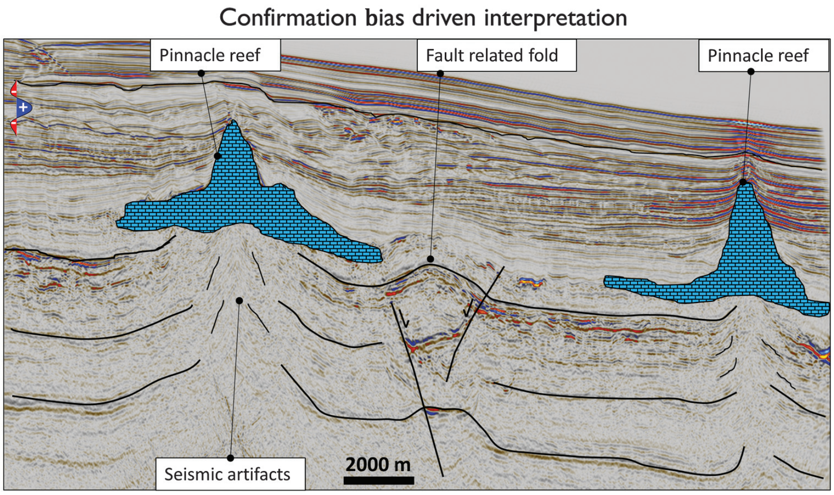

Figure 21. Interpreted vertical seismic section. Biased interpretation suggests that the mound-like features are carbonate buildups. Seismic data courtesy of NZP&M. Interpreted vertical seismic section from Figure 18a.

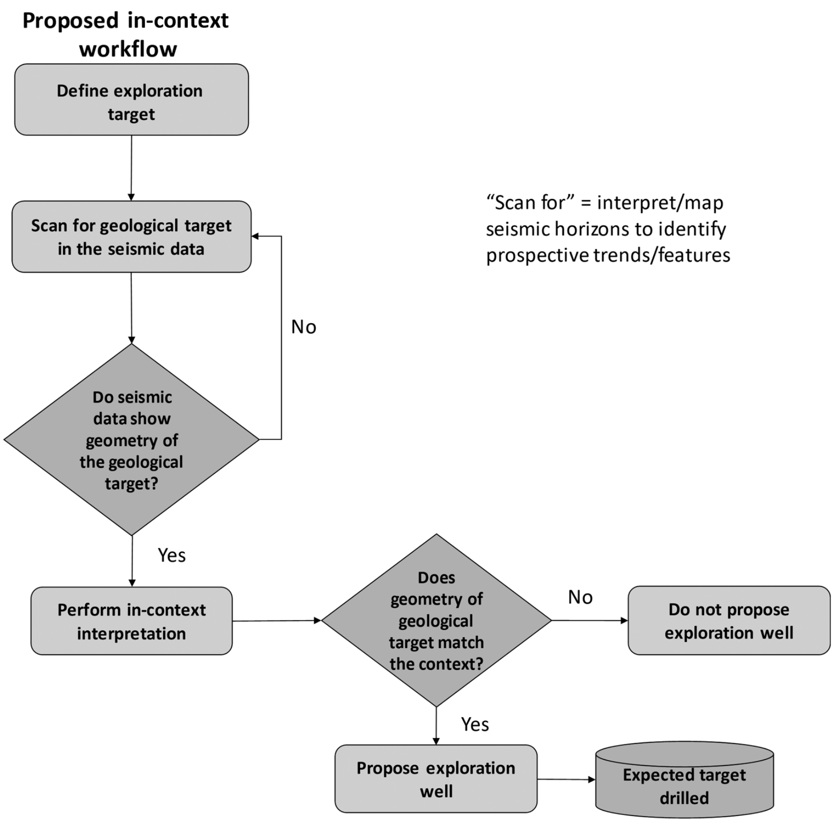

Figure 22. Proposed in-context interpretation workflow.

Conclusion

Igneous bodies can mimic the geometry and morphology of important exploration targets, such as carbonate mounds, sinuous channels, and hydrocarbon bright spots. For this reason, the interpreter cannot rely on seismic morphology and geometry alone. Whenever possible, seismic data should be complemented with other geophysical methods, such as gravity and magnetic surveys to avoid unintentionally drilling features, such as volcanic cones. An alternative and inexpensive method to avoid such pitfalls is in-context interpretation, where the interpreter examines not only the pattern of the features of interest but also the patterns of the surrounding elements. In simpler terms, we need to not only identify features we want to find, but also to identify neighboring features we do not want to find.

By understanding the context of volcanic systems, one can avoid interpreting them as something else. Important clues that help to distinguish a volcano from a carbonate mound in seismic data are the disruption of reflections immediately below the mound-like features and the igneous sills forming forced folds nearby and below the volcanic edifice. This disruption of the reflections is a common factor in old and new vintage, 2D and 3D surveys that we have analyzed in the Taranaki Basin, New Zealand.

Igneous bodies in seismic data have much in common across compressive and extensional regimes. Saucer-shaped, high-amplitude discontinuous reflections represent the real morphology of sills and should be carefully distinguished from seismic migration artifacts.

Acknowledgments

We would like to thank New Zealand Petroleum and Minerals, specifically H. Cameron for his friendly support in providing the Akira and Kora 3D seismic surveys to OU for use in research and education. Financial support for this ef-

Downloaded 02/04/19 to 68.97.115.26. Redistribution subject to SEG license or copyright; see Terms of Use at http://library.seg.org/

fort is provided by the sponsors of the Attribute-Assisted Seismic Processing and Interpretation Consortium at the University of Oklahoma. Special thanks go to D. Herron for his willingness to help and his incredible support in writing some of the final aspects of the concepts of in-context interpretation for evaluating different interpretation models. Furthermore, his constructive criticisms have undoubtedly improved the ideas expressed in this paper. Likewise, we thank our colleagues D. Lubo, G. Machado, A. Liborius, and J. McDonald for their valuable input and suggestions. We would also like to thank C. Jackson, for his insightful comments. All the 3D seismic displays were made using licenses of Petrel provided to the University of Oklahoma for research and education courtesy of Schlumberger. We would also like to thank E. Da Silva for her time and dedication with the interpretation of the Kora horizon; S. Schutter and H. Posamentier for their excellent feedback and kind support; and S. Holdford, N. Mark, P. Reynolds, N. Schofield, F. Jamaludin, Elsevier editorial, and L. Vernengo for granting permission to use their figures.

Data and materials availability

Data associated with this research are available and can be accessed via the following URL: Note: A digital object identifier (DOI) linking to the data in a general or discipline-specific data repository is strongly preferred.

References

Alves, T., K. Omosanya, and P. Gowling, 2015, Volume rendering of enigmatic high-amplitude anomalies in southeast Brazil: A workflow to distinguish lithologic features from fluid accumulations: Interpretation, **3**, no. 2, A1–A14, doi: 10.1190/INT-2014-0106.1.

Beavan, J., P. Tregoning, M. Bevis, T. Kato, and C. Meertens, 2002, Motion and rigidity of the Pacific Plate and implications for plate boundary deformation: Journal of Geophysical Research, **107**, ETG 19-1–ETG 19-15, doi: 10.1029/2001JB000282.

Bergman, S. C., J. P. Talbot, and P. R. Thompson, 1992, The Kora Miocene submarine andesite stratovolcano hydrocarbon reservoir, Northern Taranaki Basin, New Zealand: New Zealand Oil Exploration Conference Proceedings, Ministry of Commerce, 178–206.

Bischoff, A. P., A. Nicol, and M. Beggs, 2017, Stratigraphy of architectural elements in a buried volcanic system and implications for hydrocarbon exploration: Interpretation, **5**, no. 3, SK141–SK159, doi: 10.1190/INT-2016-0201.1.

Bond, C. E., A. D. Gibbs, Z. K. Shipton, and S. Jones, 2007, What do you think this is? “Conceptual uncertainty” in geoscience interpretation: GSA Today, **17**, 4–10, doi: 10.1130/GSAT01711A.1.

Cortez, M. M. M., and M. A. C. Santos, 2016, Seismic interpretation, attribute analysis, and illumination study for targets below a volcanic-sedimentary succession, Santos Basin, offshore Brazil: Interpretation, **4**, no. 1, SB37–SB50, doi: 10.1190/INT-2015-0097.1.

Delpino, D. H., and A. M. Bermudez, 2009, Petroleum systems including unconventional reservoirs in intrusive igneous rocks (sills and laccoliths): The Leading Edge, **28**, 804–811.

DeMets, C., R. G. Gordon, D. F. Argus, and S. Stein, 1994, Effect of recent revisions to the geomagnetic reversal time scale on estimates of current plate motions: Geophysical research letters, **21**, 2191–2194.

DuToit, A. I., 1920, The Karoo dolerites: Transactions Geological Society of South Africa, **33**, 1–42.

Gao, Z., W. Tian, L. Wang, Y. Shi, and M. Pan, 2017, Emplacement of intrusions of the Tarim Flood Basalt Province and their impacts on oil and gas reservoirs: A 3D seismic reflection study in Yingmaili fields, Tarim Basin, northwest China: Interpretation, **5**, no. 3, SK51–SK63, doi: 10.1190/INT-2016-0165.1.

Giba, M., A. Nicol, and J. Walsh, 2010, Evolution of faulting and volcanism in a back-arc basin and its implications for subduction processes: Tectonics, **29**, 1-18.

Giba, M., J. J. Walsh, A. Nicol, V. Mouslopoulou, and H. Seebeck, 2013, Investigation of the spatio-temporal relationship between normal faulting and arc volcanism on million-year time scales: Journal of the Geological Society, **170**, 951–962, doi: 10.1144/jgs2012-121.

Hafeez, A., S. Planke, D. A. Jerram, J. M. Millett, D. Maharjan, and T. Prestvik, 2017, Upper paleocene ultramafic igneous rocks offshore mid-Norway: Re-interpretation of the vestbrona formation as a sill complex: Interpretation, **5**, no. 3, SK103–SK120, doi: 10.1190/INT-2016-0143.1.

Hand, N., and D. Jackson, 2015, Offshore Senegal: Sud Profond 3D illustrates potential: GeoExPro, 12, https://www.geoexpro.com/articles/2015/07/offshore-senegal-sud-profond-3d-illustrates-potential, accessed 10 April 2018.

Hansen, D. M., and J. Cartwright, 2006, Saucer-shaped sill with lobate morphology revealed by 3D seismic data: Implications for resolving a shallow-level sill emplacement mechanism: Journal of the Geological Society, **3**, 509–523, doi: 10.1144/0016-764905-073.

Hayward, W. B., R. P. King, and R. E. Fordyce, 1987, Paleogeography and tectonic history of Taranaki Basin: Geological Society of New Zealand.

Holford, S. P., N. Schofield, C. A. L. Jackson, C. Magee, P. F. Green, and I. R. Duddy, 2013, Impacts of igneous intrusions on source and reservoir potential in prospective sedimentary basins along the Western Australian continental margin: West Australian Basins Symposium, Proceedings of the Petroleum Exploration Society of Australia Symposium, 1–12.

Holford, S., N. Schofield, J. MacDonald, I. Duddy, and P. Green, 2012, Seismic analysis of igneous systems in sedimentary basins and their impacts on hydrocarbon prospectivity: Examples from the southern Australian margin: The APPEA Journal, **52**, 229–252, doi: 10.1071/AJ11017.

Downloaded 02/04/19 to 68.97.115.26. Redistribution subject to SEG license or copyright; see Terms of Use at http://library.seg.org/

Holford, S. P., N. Schofield, and P. Reynolds, 2017, Subsurface fluid flow focused by buried volcanoes in sedimentary basins: Evidence from 3D seismic data, Bass Basin, offshore southeastern Australia: Interpretation, **5**, no. 3, SK39–SK50, doi: 10.1190/INT-2016-0205.1.

Infante-Paez, L., 2018, Seismic expression of igneous bodies in sedimentary basins and their impact on hydrocarbon exploration: Examples from a compressive tectonic setting, Taranaki Basin, New Zealand: Ph.D. dissertation, The University of Oklahoma.

Infante-Paez, L., and K. J. Marfurt, 2017, Seismic expression and geomorphology of igneous bodies: A Taranaki Basin, New Zealand, case study: Interpretation, **5**, no. 3, SK121–SK140, doi: 10.1190/INT-2016-0244.1.

Jackson, C. A. L., N. Schofield, and B. Golenkov, 2013, Geometry and controls on the development of igneous sill-related forced folds: A 2-D seismic reflection case study from offshore southern Australia: Bulletin of the Geological Society of America, **125**, 1874–1890, doi: 10.1130/B30833.1.

King, P. R., and G. P. Thrasher, 1992, Post-Eocene development of the Taranaki Basin, New Zealand: Convergent overprint of a passive margin: Geology and Geophysics of Continental Margins, **53**, 93–118.

King, P. R., and G. P. Thrasher, 1996, Cretaceous Cenozoic geology and petroleum systems of the Taranaki Basin, New Zealand: Institute of Geological and Nuclear Sciences Limited, Institute of Geological and Nuclear Sciences 2.

Klarner, S., and O. Klarner, 2012, Identification of paleovolcanic rocks on seismic data: Updates in volcanology: A comprehensive approach to volcanological problems: InTech.

Klarner, S., B. Ujetz, R. Fontana, and J. Altenkirch, 2006, Seismic signature of Upper Cretaceous volcanics: Santos Basin, Brazil: 68th Annual International Conference and Exhibition, EAGE, Extended Abstracts, 105.

Krueger, J., and D. Funder, 2004, Towards a balanced social psychology: Causes, consequences and cures for the problem-seeking approach to social behavior and cognition: Behavioral and Brain Sciences, **27**, 313–327.

Liborius-Parada, A., and D. Tazzo, 2012, Petrografía de la aureola de contacto de la granodiorita de El Carmen en las adyacencias del pico El Águila-vía Piñango, edo. Mérida, Venezuela: GEOS Venezuelan Journal of Earth Sciences, **42**, 72–76.

Magee, C., E. Hunt-Stewart, and C. A. L. Jackson, 2013, Volcano growth mechanisms and the role of sub-volcanic intrusions: Insights from 2D seismic reflection data: Earth and Planetary Science Letters, **373**, 41–53, doi: 10.1016/j.epsl.2013.04.041.

Magee, C., C. A.-L. Jackson, J. P. Hardman, and M. T. Reeve, 2017, Decoding sill emplacement and forced fold growth in the Exmouth Sub-basin, offshore northwest Australia: Implications for hydrocarbon exploration: Interpretation, **5**, no. 3, SK11–SK22, doi: 10.1190/INT-2016-0133.1.

Magee, C., C. A. L. Jackson, and N. Schofield, 2014, Diachronous sub-volcanic intrusion along deep-water margins: Insights from the Irish Rockall Basin: Basin Research, **26**, 85–105, doi: 10.1111/bre.12044.

Magee, C., J. D. Muirhead, A. Karvelas, S. P. Holford, C. A.-L. Jackson, I. D. Bastow, N. Schofield, C. T. Stevenson, C. McLean, W. McCarthy, and O. Shtukert, 2016, Lateral magma flow in mafic sill complexes: Geosphere, **12**, 809–841, doi: 10.1130/GES01256.1.

Mark, N. J., N. Schofield, S. Pugliese, D. Watson, S. Holford, D. Muirhead, R. Brown, and D. Healy, 2018, Igneous intrusions in the Faroe Shetland basin and their implications for hydrocarbon exploration; new insights from well and seismic data: Marine and Petroleum Geology, **92**, 733–753, doi: 10.1016/j.marpetgeo.2017.12.005.

McLean, C. E., N. Schofield, D. J. Brown, D. W. Jolley, and A. Reid, 2017, 3D seismic imaging of the shallow plumbing system beneath the Ben Nevis Monogenetic volcanic field: Faroe-Shetland Basin: Journal of the Geological Society, **174**, 468–485, doi: 10.1144/jgs2016-118.

Miles, A., and J. Cartwright, 2010, Hybrid flow sills: A new mode of igneous sheet intrusion: Geology, **38**, 343–346, doi: 10.1130/G30414.1.

Naviset, S., C. K. Morley, D. H. Naghadeh, and J. Ghosh, 2017, Sill emplacement during rifting and inversion from three dimensional seismic and well data, Phitsanulok Basin, Thailand: Geosphere, **13**, 2017–2040, doi: 10.1130/GES01466.1.

Neall, V. E., R. B. Stewart, and I. E. M. Smith, 1986, History and petrology of the Taranaki volcanoes: Royal Society of New Zealand Bulletin, **23**, 251–263.

Pena, V., S. Chávez-Pérez, M. Vázquez-García, and K. J. Marfurt, 2009, Impact of shallow volcanics on seismic data quality in Chicontepec Basin, Mexico: The Leading Edge, **28**, 674–679.

Planke, S., E. Alvestad, and O. Eldholm, 1999, Seismic characteristics of basaltic extrusive and intrusive rocks: The Leading Edge, **18**, 342–348.

Rabbel, O., O. Galland, K. Mair, I. Lecomte, K. Senger, J. B. Spacapan, and R. Manceda, 2018, From field analogues to realistic seismic modeling: A case study of an oil-producing andesitic sill complex in the Neuquén Basin, Argentina: Journal of the Geological Society, **175**, 580–593, doi: 10.1144/jgs2017-116.

Reynolds, P., N. Schofield, R. J. Brown, and S. P. Holford, 2018, The architecture of submarine monogenetic volcanoes: Insights from 3D seismic data: Basin Research, **30**, 437–451, doi: 10.1111/bre.12230.

Rodriguez Monreal, F., H. J. Villar, R. Baudino, D. Delpino, and S. Zencich, 2009, Modeling an atypical petroleum system: A case study of hydrocarbon generation, migration and accumulation related to igneous intrusions in the Neuquen Basin, Argentina: Marine and Petroleum Geology, **26**, 590–605, doi: 10.1016/j.marpetgeo.2009.01.005.

Sarkar, S., and K. J. Marfurt, 2017, Effect of volcanic bodies on hydrocarbon reservoirs in the northeastern part of

Downloaded 02/04/19 to 68.97.115.26. Redistribution subject to SEG license or copyright; see Terms of Use at http://library.seg.org/

Downloaded 02/04/19 to 68.97.115.26. Redistribution subject to SEG license or copyright; see Terms of Use at http://library.seg.org/

the Chicontepec Foredeep, Mexico: Interpretation, **5**, no. 3, SK1–SK10, doi: 10.1190/INT-2016-0110.1.

Schmiedel, T., S. Kjoberg, S. Planke, C. Magee, O. Galland, N. Schofield, C. A.-L. Jackson, and D. A. Jerram, 2017, Mechanisms of overburden deformation associated with the emplacement of the Tulipan sill, mid-Norwegian margin: Interpretation, **5**, no. 3, SK23–SK38, doi: 10.1190/INT-2016-0155.1.

Schofield, N., S. Holford, J. Millett, D. Brown, D. Jolley, S. R. Passey, D. Muirhead, C. Grove, C. Magee, J. Murray, M. Hole, C. A.-L. Jackson, and C. Stevenson, 2017, Regional magma plumbing and emplacement mechanisms of the Faroe-Shetland sill complex: Implications for magma transport and petroleum systems within sedimentary basins: Basin Research, **29**, 41–63, doi: 10.1111/bre.12164.

Senger, K., J. Millett, S. Planke, K. Ogata, C. H. Eide, M. Festøy, O. Galland, and D. A. Jerram, 2017, Effects of igneous intrusions on the petroleum system: A review: First Break, **35**, 47–56.

Thomson, K., 2007, Determining magma flow in sills, dykes and laccoliths and their implications for sill emplacement mechanisms: Bulletin of Volcanology, **70**, 183–201, doi: 10.1007/s00445-007-0131-8.

Kurt J. Marfurt began his geophysical career teaching geophysics and contributing to an industry-supported consortium on migration, inversion, and scattering (project MIDAS) at Columbia University's Henry Krumb School of Mines in New York City. In 1981, he joined Amoco's Tulsa Research Center and spent the next 18 years leading research efforts in modeling, migration, signal analysis, basin analysis, seismic attribute analysis, reflection tomography, seismic inversion, and multicomponent data analysis. In 1999, he joined the University of Houston as a professor in the Department of Geosciences and as a director of the Allied Geophysics Laboratories. He is currently a member of the Geophysical Societies of Tulsa and Houston, SEG, EAGE, AAPG, AGU, and SIAM, and he serves as the editor of *Interpretation*. His current research activity includes prestack imaging, velocity analysis and inversion of converted waves, computer-assisted pattern recognition of geologic features on 3D seismic data, and interpreter-driven seismic processing. His research interests include seismic signal analysis, 3D seismic attributes, seismic velocity analysis, subsurface imaging, and multicomponent data analysis.

Lennon Infante received a bachelor's degree in geophysical engineering from Simon Bolivar University, Venezuela. He completed his master's degree in geology from The University of Oklahoma under Roger Slatt. He completed his doctorate degree in geophysics from The University of Oklahoma in 2018. He was mentored by AAPG member Kurt Marfurt. His research interests include seismic interpretation, reservoir characterization, and seismic expression of igneous rocks.